frontiers | Frontiers in Environmental Science

TYPE Original Research
PUBLISHED 03 June 2024
DOI 10.3389/fenvs.2024.1381781

OPEN ACCESS

EDITED BY
Giuseppe Mancuso,
University of Bologna, Italy

REVIEWED BY
Mathieu Nsenga Kumwimba,
Chinese Academy of Sciences (CAS), China
Francesco Chioggia,
University of Bologna, Italy

*CORRESPONDENCE
Shunyao Zhuang,
syzhuang@issas.ac.cn

RECEIVED 04 February 2024
ACCEPTED 13 May 2024
PUBLISHED 03 June 2024

CITATION
Zhang Y, Gao J, Li Q and Zhuang S (2024), Reduction of nitrogen loss in runoff from sloping farmland by a ridged biochar permeable reactive barrier with vegetated filter strips. *Front. Environ. Sci.* 12:1381781. doi: 10.3389/fenvs.2024.1381781

Reduction of nitrogen loss in runoff from sloping farmland by a ridged biochar permeable reactive barrier with vegetated filter strips

Yuhe Zhang[1,2], Jianshuang Gao[1], Qiang Li[3] and Shunyao Zhuang[1]*

[1]Institute of Soil Science, Chinese Academy of Sciences, Nanjing, China, [2]College of Modern Agricultural Sciences, University of Chinese Academy of Sciences, Beijing, China, [3]Department of Natural Sciences, University of Houston-Downtown, Houston, TX, United States

Introduction: Eutrophication due to nitrogen (N) loss from sloping farmland has a high risk in the Three Gorges Reservoir. Biochar and vegetated filter strips (VFS) are used to control nutrient runoff and increase soil water-holding capacity, soil nutrient retention, and crop yield. However, surface biochar application has limited ability to control N loss, especially from sloping farmland.

Methods: In this study, different widths of ridged biochar permeable reactive barrier (RB-PRB) with VFS were employed to intercept N loss in runoff from sloping farmland. Adsorption characteristics of biochar for nitrate and ammonium N were evaluated using isothermal and kinetic adsorption models before field experiments. N index values for ammonium (NH_4^+), nitrate (NO_3^-), dissolved N (DTN), particulate N (PN), and total N (TN) lost through runoff were monitored from April 2019 to January 2020.

Results: NO_3^- and NH_4^+ sorption on biochar was predominantly physical adsorption with a maximum capacity of 4.51 and 4.12 mg g^{-1}, respectively. During the research period, the dominant transportation pathway of N loss involved dissolved total N movement through subsurface flow, which accounted for 65.55% of the total loss. TN loss for CK was 1954 g·hm^{-2}, while RB-PRB and VFS decreased N loss from sloping farmland by 36.7%. The interception efficiency of RB-PRB was highest at 0.3 m width. VFS successfully intercepted particulate N and reduced it by 32.75%. In terms of soil nutrients, the RB-PRB and VFS interventions led to a substantial 41.69% increase in the TN content of the soil at a 0.4 m width.

Discussion: The findings suggest that biochar has a favorable adsorption effect on NH_4^+ and NO_3^-, an appropriate width of RB-PRB with VFS could effectively reduce nitrogen loss from sloping farmland. Simultaneously, it enhances the water and fertilizer retention capacity of sloping cropland soil; however, the long-term implications necessitate further validation.

KEYWORDS

sloping farmland, nitrogen loss, ridged biochar permeable reactive barrier, vegetated filter strips, eutrophication, agricultural runoff

1 Introduction

Sloping farmland is the dominant type of arable land in hilly purple soil areas in Southwest China (Guo et al., 2019). Within these areas, gently sloping farmland (15°–25°) has a high percentage of 23.8% of the country's total farmland area. Precipitation events can result in the transport of large quantities of nutrients via overland flow and interflow, ultimately leading to the introduction of these nutrients into the Three Gorges Reservoir (TGR), which is the largest reservoir in China (Liu et al., 2016). Nitrogen (N), serving as a pivotal element in soil ecosystem nutrient cycling, exerts a profound influence on soil quality and regulates nutrient dynamics. Being indispensable for plant growth and soil fertility enhancement, soil N loss from soil via runoff can result in significant land degradation and in diminished land productivity (Li et al., 2022). In cases of N deficiency in the soil, plant growth and reproduction are impeded, leading to decreased vegetation cover and heightened soil erosion (Peng et al., 2019). Moreover, Eutrophication and ecological harm can occur when N leached from farmland enters water bodies, making it a major contributor to non-point source pollution from agriculture (Ibrikci et al., 2015). Notably, the issue of N surface source pollution through soil erosion is particularly acute in southwestern China, because of the shallow soil depth and limited fertility retention capacity of cultivated land on purple soil sloping farmland (Wang et al., 2023). Therefore, controlling N loss from sloping farmland surrounding the TGR watershed is important and urgent.

N loss from farmland has received significant global attention, and specialised research was conducted: it was assessed that, in general, soil N is lost from farmland through volatilization, vertical leaching, runoff, and sediment transport (Zhao et al., 2015). Furthermore, the main routes for nutrient and sediment loss of nitrogen from sloping farmland are through runoff and soil erosion (Lemma et al., 2017; Tuo et al., 2018). Soil N can enter the runoff through two pathways: firstly, nutrients from chemical or organic fertilizers may dissolve in the soil solution and then be carried by surface runoff via water exchange. Secondly, N may adsorb onto the soil particle surface and be transported by runoff through desorption, which may also result in sediment erosion (Wang et al., 2022). While numerous studies have concentrated on surface runoff (Libutti and Monteleone, 2017; Lee et al., 2018), only a few have explored subsurface flow, which is critical in runoff and which contributes to groundwater and reservoir contamination (Holly et al., 2018). As reported, subsurface flow can account for 63% of total runoff and is the main driver of N leaching in hilly regions (Zhu et al., 2009). Therefore, it is critical to find a way to control N loss via subsurface runoff from sloping land surrounding the TGR.

Various techniques are used to prevent and control soil nutrient loss. Based on a meta-analysis, Shen et al. reported that the overall effect of ecological ditches was a 38.7% reduction in total nitrogen (TN), which indicates the great application potential of ditches in removing TN (Shen et al., 2021). However, ecological ditches do not perform well at low temperatures, and they may even become N sources (Wang et al., 2017). Luo et al. reported that the average removal rate of total nitrogen (TN) from agricultural surface runoff on farmland in constructed wetlands was 29.64% (Luo et al., 2022). Additionally, during heavy rainfall events, this method does not have a good effect to the elevated N concentrations (Wei et al., 2020). Vegetated filter strips (VFS), designated areas of land intended to create a buffer between agricultural land and ecologically significant aquatic or terrestrial environments. They demonstrated efficacy in intercepting agricultural non-point-source pollution before it enters a water body (Prosser et al., 2020; Tang et al., 2021). Research consistently demonstrates that VFS can efficiently capture a substantial portion of the total phosphorus and nitrate load in field runoff, preventing its entry into surface water (Janssen et al., 2018; Lyu et al., 2021). Notably, the VFS contributes to the reduction of surface runoff and associated solute and particle transport. However, VFS application is still limited due to a high requirement of large reactor volumes or large areas of land (Gene et al., 2019).

Biochar is a type of charcoal that is produced from organic materials through a process called pyrolysis, and is considered a favorable soil amendment. When applied in appropriate amounts in agricultural production, it can boost soil microbial populations, enhance soil pH, stimulate soil enzyme activity, increase porosity and macro-aggregates, expand soil nutrient availability, and facilitate soil infiltration and plant absorption of accessible N (Wu et al., 2018; Chen et al., 2020). Meanwhile, apoplastic matter from growing vegetation also contributes to the increase in TN of soil (Wu et al., 2022). However, there have been some negative comments in previous investigations. The entrainment of NH_4^+ biochar particles was washed out by the surface flow and caused led to increased NH_4^+ loss fluxes, due to their minute size and low density (Huang et al., 2020). Since for sloping farmland N is mainly lost through runoff caused by rainfall, the interception of N by surface-applied biochar is believed to be limited (Wu et al., 2022). In conclusion, the extent of runoff prevention and control technologies is limited by land use, topography and other factors, and therefore, there is an urgent need for more effective and high-capacity measures for removing N in rainfall runoff from sloping farmland.

Based on the characteristics of runoff from sloping farmland surrounding the TGR, a new *in situ* remediation technique, ridged biochar permeable reactive barrier (RB-PRB) combined with VFS, was explored for preventing N loss from sloping farmland (Losacco et al., 2021; Chen et al., 2022). This composite barrier strip adsorbs nitrogen lost in runoff through the RB-PRB, while the VFS reduces the migration of particulate matter and total dissolved nitrogen. Nevertheless, the specific adsorption mechanism of this composite interception zone remains ambiguous, and its interception efficacy in practical agricultural systems is yet undetermined. The method may be effective for intercepting mid-loam flow in purple soils during heavy rainfall events, but its effectiveness at blocking N was unclear. Consequently, this study encompassed an indoor simulated adsorption test and an *in situ* evaluation of RB-PRB with VFS implemented in the TGR area. The primary aim was to evaluate the effects of RB-PRB with VFS on N loss in runoff based on the characteristics of N adsorption on biochar. The results can provide a practical solution and scientific support for mitigating N losses from sloping farmland in the Three Gorges Reservoir area.

2 Materials and methods

2.1 Study site location and climate

Field experiments were performed at Shipanqiu sub-basin (30°24'~30°30'N, 108°08'~108°12'E), situated in Shibao Town, Zhong County, Chongqing city of China. This sub-basin is adjacent to the

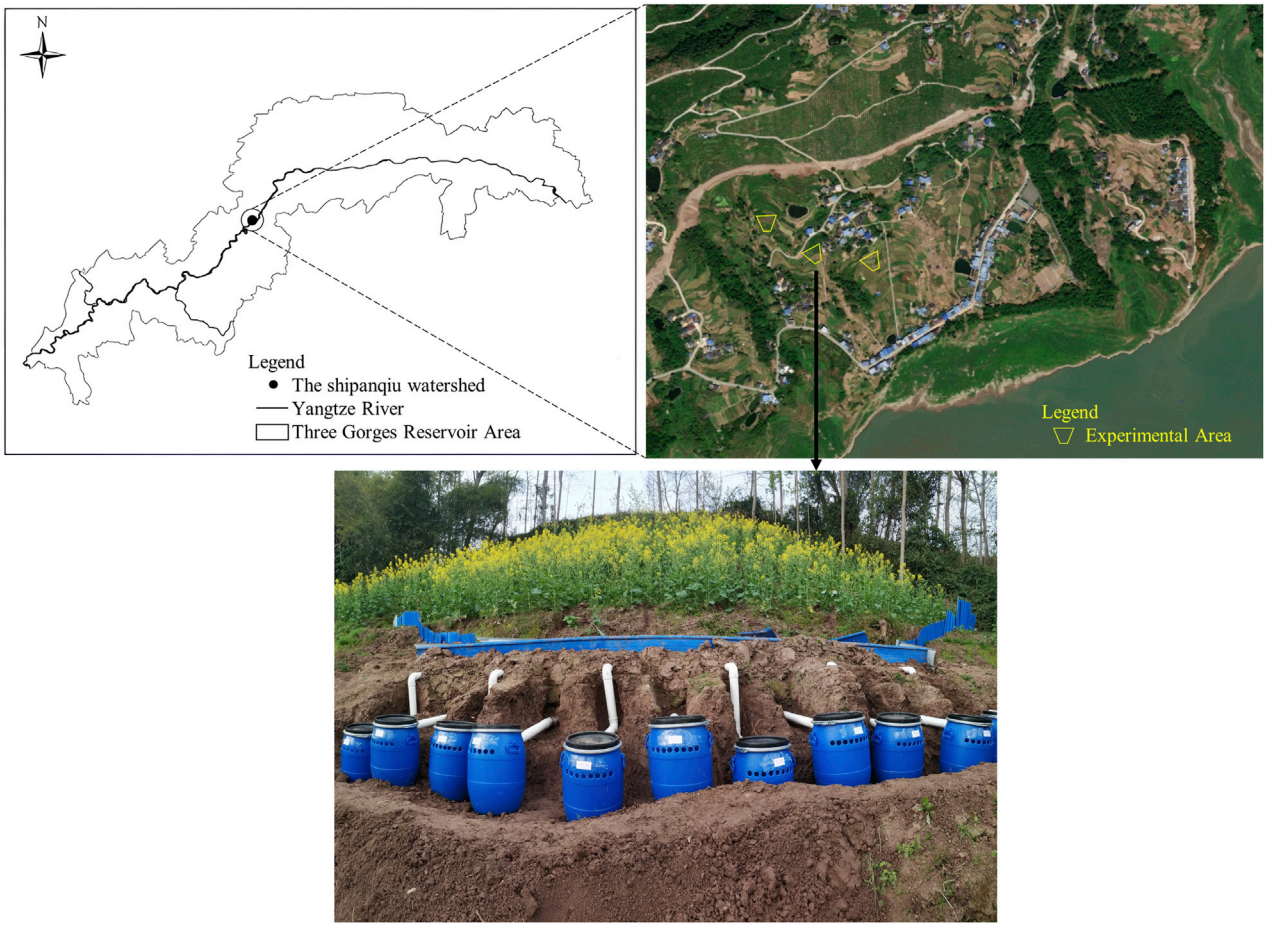

FIGURE 1
Location of the experimental area and diagram of runoff plot on sloping farmland.

middle reaches of the Yangtze River, and the basin outlet confluence directly enters the Three Gorges Reservoir water body. Figure 1 shows the location of the test site in the Three Gorges reservoir Area. The study area features a hilly mountainous landscape with a humid monsoon climate type. The basin exhibits an average annual precipitation ranging from 1,000 to 1,300 mm. Rainfall occurs predominantly during the rainy season, which spans from April to October each year and accounts for around 70% of the annual precipitation. Notably, heavy rainfall concentrates between June and August annually. The weather data were provided by the weather station in the Experimental Station for Soil and Water Conservation and Environmental Research in the Three Gorges Reservoir Region, Chinese Academy of Sciences.

The soils investigated in this study are predominantly classified as purple soils, formed on purple or purplish-red sandstone and shale formations. Purple soil is deemed to be highly representative of the sloping land types found within the Three Gorges Reservoir Area due to its shallow bedrock, limited soil depth, low fertility retention capacity, and high susceptibility to erosion. The soil physicochemical properties of purple soil in sloping farmland were measured at the beginning of the experiment. The pH of the soils was measured with a pH-measuring instrument (FiveEasy Plus pH meter FP20, Mettler Toledo Co., Ltd., Shanghai, China) in a soil-water suspension (1:2.5, *w*/*v*). The soil bulk density was determined using the cutting ring method. Water content was determined by weighing method. Soil organic carbon (SOC) was determined using the high-temperature exothermic–potassium dichromate oxidation-volumetric method (James and Haby, 1971). Total N (TN) was determined using the Kjeldahl method. The soil alkali-hydrolyzed N (AN) was determined using the alkaline diffusion method (Tsiknia et al., 2014). Nitrate nitrogen (NO_3^--N) and ammonium nitrogen (NH_4^+-N) were analyzed by using the sulfanilamide colorimetry and indophenol blue colorimetry, respectively (Dai et al., 2023). The molybdenum-antimony colorimetric method was used to measure total P (TP) and available P (AP) (Liu et al., 2017). Total potassium (TK) and available K (AK) determined using a flame photometer (FP640, Shanghai Precision & Scientific Instrument Inc., Shanghai, China) (Yanu and Jakmunee, 2015). The properties of the soils are listed in Supplementary Table S1. In this region, the standard crop rotation involves rotating summer maize and winter rape.

2.2 Batch experiment

Isothermal adsorption tests and kinetic adsorption tests were set up in laboratory experiments. Biochar (0.2 g) was put in a 250 mL

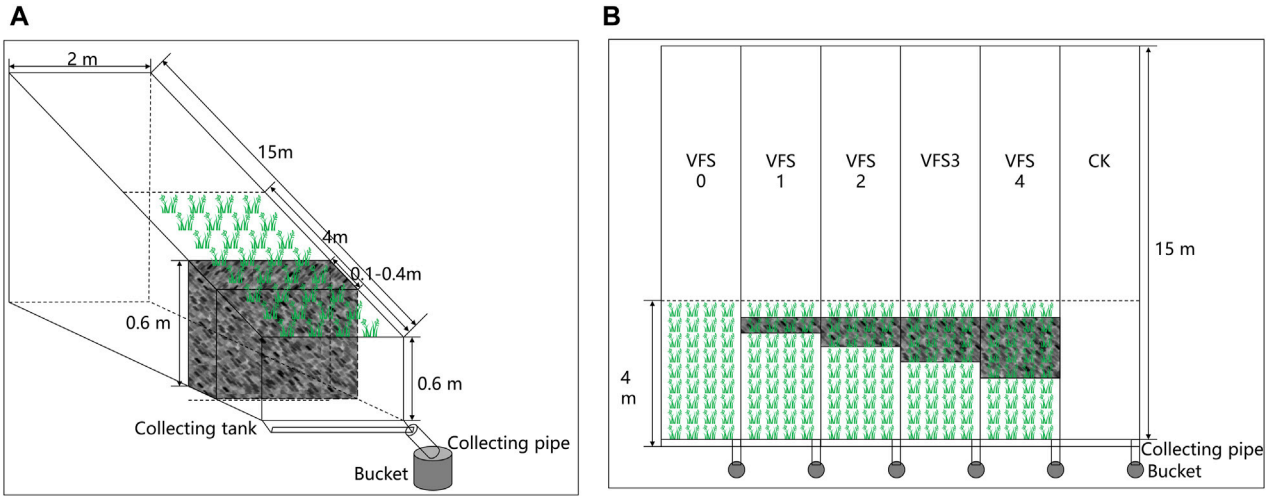

FIGURE 2
Side sketch **(A)** and Planar sketch **(B)** of the experimental design for the sloping farmland runoff plots.

conical flask, and then 100 mL of NH_4Cl and $NaNO_3$ solutions (0, 10, 20, 40, 60, 80, and 100 mg L^{-1}) were added. To prevent evaporation of water, the conical flasks were sealed with plastic wrap, and flasks were shaken in a water bath shaking chamber at 25°C ± 1 °C with an oscillation frequency of 150 rpm for adsorption. After shaking for 48 h, 10 mL of each suspension was removed, filtered through a 0.45 μm Polyethersulfone (PES) filter membrane to prevent the influence of biochar on absorbance, and the content of NO_3^--N and NH_4^+-N in solution was determined by colorimetric method (Ruan et al., 2016). Each treatment was repeated in triplicate.

Similarly, in the absorption kinetic experiment, a quantity of 0.2 g of biochar was blended with 100 mL of a solution containing 100 mg L^{-1} NO_3^--N and 100 mg L^{-1} NH_4^+-N, with the contact duration ranging from 0 to 48 h. The experimental parameters such as stirring rate, temperature, and the quantification of NO_3^--N and NH_4^+-N remained consistent with those employed in the absorption isotherm investigation.

2.3 Field experiment

Runoff plots were selected and designed for this study based on the hydrological characteristics of sloping farmland. Each plot, representative of the study area, was built as a 72 m^2 cell (12 m × 6 m in length and width), with a 15° slope and soil depth of 60 cm. A randomized design was used to allocate six treatments, each with three replicates. Treatments included a plot without RB-PRB and VFS as a control (CK), VFS0 (without RB-PRB), VFS1 (with RB-PRB in a width of 0.1 m), VFS2 (0.2 m), VFS3 (0.3 m) and VFS4 (0.4 m).

To prevent water and nutrient exchange between plots, soils in each plot were lined with plastic film at the bottom and sides, and stainless steel plates was inserted into the soil at a depth of 40–60 cm to isolate each plot individually (Figure 2). At the downslope edge of every plot, some collection pipe and collecting tanks were set up to collect runoff and sediment for measurement. Water samples from the bucket were regularly taken and chemically analyzed.

Biochar obtained from pyrolysis of moso bamboo (*Phyllostachys edulis*) that was at least 4 years old and produced at 800°C was utilized in this study (Suichang Shenlonggu Carbon Industry Co. Ltd., Lishui, China). BET characterization results showed that, the average specific surface area, total hole volume, and average pore size of the biochar were 161.08 m^2 g^{-1}, 0.0795 cm^3 g^{-1}, and 19.75 Å, respectively.

Land use and management practices applied within this study are consistent with local customs. Maize and oilseed rape are used in a standard crop rotation, where oilseed rape is typically sown in November and harvested in April of the subsequent year; maize is sown in May and harvested in September. Depending on the local conditions, maize and oilseed rape was grown using the burrowing and light tillage method, with plant spacing and row spacing of 40 cm and 60 cm, respectively. Conventional weed and pest control practices were implemented in the region. Hybrid giant Napier (*Pennisetum* × *sinese*) was planted in the vegetated filter strip area. Fertilizer application followed common practices among local farmers, with a total of 450 kg N ha^{-1} (urea, N-eq 46%), 240 kg P_2O_5 ha^{-1} (superphosphate, P_2O_5-eq 12%), and 225 kg K_2O ha^{-1} (potassium sulfate, K_2O-eq 52%) applied. All of the superphosphate and potassium sulfate were applied as basal fertiliser. 80% of the urea was applied as a base fertiliser and 20% as supplemental fertilizer. (Huang et al., 2018).

2.4 Sample analyses

For soil mid-flow and sediment sample collection, runoff collection buckets were placed in the collection tank below the runoff plots before starting the test, and rainfall and runoff volumes were recorded at the same time. In each test, at the end of the runoff period, the runoff water in each bucket was fully stirred using a clean PVC board. Water samples were collected at specified intervals into 500 mL polyethylene bottles and stored at 4°C until analysis. Concentrations of N fractions were measured within 48 h of collection. The water samples were mixed thoroughly prior to each measurement.

After mixing, the water samples were adjusted to a neutral pH of 7 and subjected to digestion with $K_2S_2O_8$ solution. TN was quantified using UV-Vis spectrophotometry on a UV-5800 (Shanghai Metash, City, China). The remaining water samples were filtered through a 0.45 μm PES filter membrane and digested with $K_2S_2O_8$ solution. Total dissolved nitrogen (TDN), NO_3^--N, and NH_4^+-N were analyzed using an AA1 continuous flow auto-analyzer (Seal, City, Germany). Particulate nitrogen (PN) was determined by subtracting TDN from TN. To study the effect of RB-PRB and VFS on soil nutrients in sloping arable land, soil was sampled from runoff plots under each treatment in each sloping arable land in April, July, October and January of the following year. TN in the soil was determined using the Kjeldahl method.

2.5 Data analysis and statistics

In order to optimize the use of adsorbents, previous studies have suggested modeling interactions between biochar and N during the adsorption process (He et al., 2023). NO_3^--N, and NH_4^+-N adsorption kinetics were investigated in this study to explore the mechanisms of the thermodynamic and dynamic adsorption of NO_3^--N and NH_4^+-N on biochar. The Eqs 1–4 kinetics models were employed to evaluate NO_3^--N and NH_4^+-N adsorption on different biochars. These models are listed as follows (Xiang et al., 2021):

$$\text{Langmuir equation: } \frac{c_e}{q_e} = \frac{1}{q_{max}b} + \frac{1}{q_{max}} \cdot c_e \quad (1)$$

$$\text{Freundlich equation: } ln\, q_e = ln\, K_f + 1/n \cdot ln\, c_e \quad (2)$$

$$\text{Pseudo-first-order (Lagergren) model: } q_t = q_e\left(1 - e^{-k_1 t}\right) \quad (3)$$

$$\text{Pseudo-second-order model: } q_t = q_e^2 k_2 t / \left(1 + q_e k_2 t\right) \quad (4)$$

where c_e (mg·L^{-1}) is the concentration of NO_3^--N, and NH_4^+-N in the mixture at adsorption equilibrium, q_e (mg·g^{-1}) is the adsorbed amount of NO_3^- and NH_4^+ at equilibrium, q_{max} (mg·g^{-1}) is the maximum adsorption amount of NO_3^--N, and NH_4^+-N, b (L·mg^{-1}) is the Langmuir adsorption constant, K_f is a constant representing the adsorption capacity.

1/n is a constant describing the adsorption strength, q_t (mg·g^{-1}) is the amount of NO_3^--N, and NH_4^+-N adsorbed at time t, k_1 (h^{-1}) and k_2 (g·mg^{-1}·h^{-1}) are the rate constants of pseudo-first-order and pseudo-second-order adsorption, respectively, and t (h) is the time of sampling.

The runoff flux of subsurface flow from rainfall events was calculated by the Eq. 5, which was proposed and modified by Peng et al. (2016):

$$\text{Runoffflux (mm)} = \frac{V}{A} \times 1000 \quad (5)$$

where V represents the volume of runoff fluid collected (L), and A denotes the surface area of each test block (m^2).

N fraction loss flux via subsurface flow was calculated through the Eq. 6 (Zhu et al., 2009):

$$Q = \sum_i^n C_i \times q_i \times 10 \quad (6)$$

where Q represents N loss flux throughout the experimental period (g·ha^{-1}), C_i represents the concentration of a particular N fraction for each single rainfall event (mg·L^{-1}), q_i represents the runoff flux (mm), and $i = 1$ to n is the total number of rainfall events during the experimental period.

SPSS 24.0 (SPSS, Chicago, USA) was employed to conduct statistical analysis. ANOVA was used to investigate treatment effects, while paired T-tests were performed to compare nitrogen loss difference between interflow runoff. Results with a p-value of less than 0.05 were considered statistically significant. Moreover, standard errors were calculated with Excel 2019.

3 Results

3.1 Adsorption characteristics of nitrogen on biochar

Langmuir and Freundlich models were used to fit the adsorption data of NO_3^--N and NH_4^+-N on biochar, respectively, in order to investigate the isotherms. Figure 3 presents the fitting curves of the models, and the corresponding parameters can be found in Table 1. The results show the adsorption of NO_3^--N, and NH_4^+-N by biochar increased with the addition of solute concentration and then stabilized slowly. The adsorption of NO_3^--N (6.04 mg g^{-1}) was slightly greater than the adsorption of NH_4^+-N (4.10 mg g^{-1}) as fitted by the Langmuir model. The Langmuir equation provided a better fit for the sorption of NO_3^--N (R^2 = 0.9588) and NH_4^+-N (R^2 = 0.9673) on biochar compared to the Freundlich equation (R^2 = 0.8812, R^2 = 0.9450, respectively), as indicated by the correlation coefficient (R^2). Moreover, within the framework of the Freundlich model, the uptake constants 1/n for NO_3^--N and NH_4^+-N were determined to be 0.4850 and 0.5090, respectively (both values being less than 1).

The effect of contact time on N adsorption by biochar was investigated for 48 h. The adsorption of NO_3^--N, and NH_4^+-N by biochar showed a trend of fast and then slow (Figure 4). In the initial stages (0.5–12 h), the amount of adsorption NO_3^--N, and NH_4^+-N increased significantly over time, from 1.52 to 1.32 mg g^{-1} to 4.36 and 3.96 mg g^{-1}, respectively. In the subsequent adsorption phase (12–48 h), the adsorption rate slowed down significantly, the adsorption amount remained almost unchanged, from 4.36 to 3.96 mg g^{-1} to 4.51 and 4.12 mg g^{-1}, respectively. The fitted kinetic parameters are listed in Table 2. The apparent sorption equilibrium of N adsorption on the selected adsorbents was achieved after 12 h. Both models of pseudo-first-order and pseudo-second-order provided a good fit to the adsorption data, as confirmed by the regression coefficient (R^2).

3.2 Nitrogen content in runoff from sloping land over time

Figure 5 shows the rainfall within the runoff plots of sloping farmland and the temporal variation of TN and TDN concentrations lost in runoff from the RB-PRB and VFS interception areas for the corresponding rainfall amounts. Seasonal variation in rainfall can be clearly seen, which in turn correlates significantly with seasonal variation in TN and TDN content in runoff. The trend of high N loss in summer and low loss in spring was observed. The greatest TN loss reached 81.46 mgL^{-1}

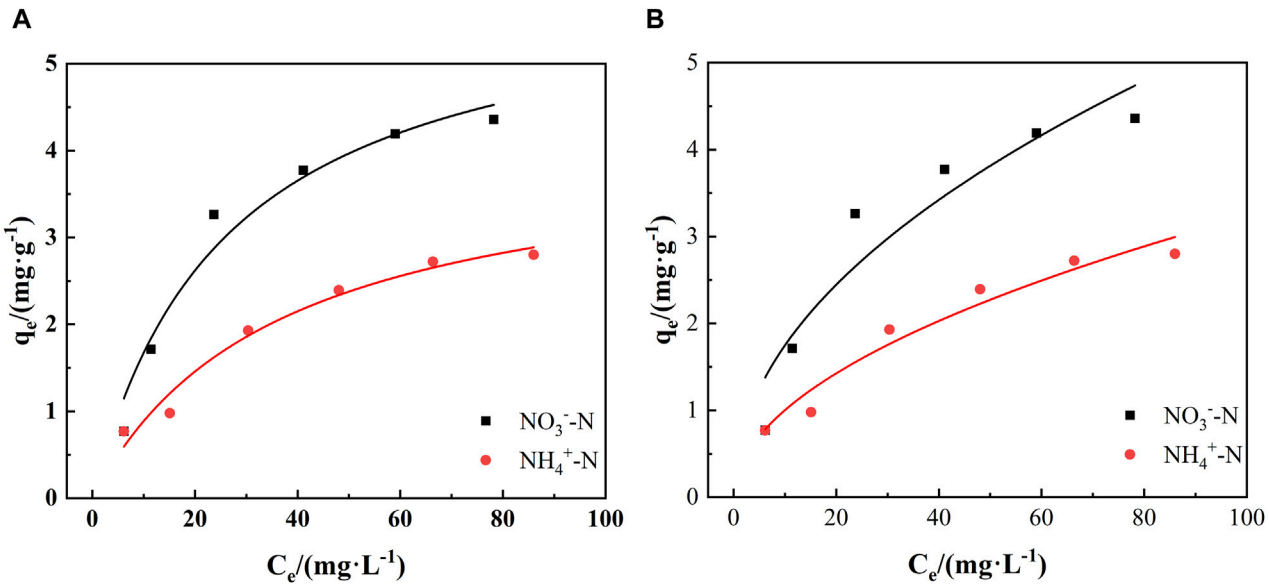

FIGURE 3
Isothermal adsorption of NO_3^--N and NH_4^+-N on biochar fitted using Langmuir **(A)** and Freundlich **(B)** models.

TABLE 1 Fitting parameters of NO_3^--N and NH_4^+-N adsorption on biochar.

	Langmuir			Freundlich		
	b	q_m/mg·g^{-1}	R^2	K_f	*1/n*	R^2
NO_3^--N	0.0383	6.04	0.9588	0.5718	0.4850	0.8812
NH_4^+-N	0.0275	4.10	0.9673	0.3102	0.5090	0.9450

on August 6. The TN and TDN concentrations in runoff also peaked in September when the arable crops were replaced. TN loss with only VFS0 for interception was 1.52–64.24 mg L^{-1}, significantly lower than TN loss from controls (2.87–81.45 mg L^{-1}). Meanwhile, TN and TDN in runoff decreased as the RB-PRB width increased. However, when the RB-PRB width was >0.3 m, the interception effect did not change significantly.

3.3 Nitrogen interception from sloping farmland

The interception of various forms of N by RB-PRB with VFS from sloping farmland is shown in Figure 6. Loss of TN clearly decreased with increasing width of RB-PRB. Slope runoff N was mainly in the form of particulate N (PN) and TDN. After the establishment of runoff plots in April 2019, TN loss from controls was 1954 g·hm^{-2}. Of this amount, the TDN loss was 1,281 g hm^{-2} land, accounting for 65.55% of the total loss, indicating that TDN was the main form of N loss. Compared with CK, the interception efficiency of VFS0, a treatment with only VFS, was 32.75% for PN, but only 15.56% for TN, which indicates that VFS could effectively intercept PN. Compared with VFS0, interception of TN was significantly higher in VFS2, VFS3, and VFS4 treatments with increasing RB-PRB width, which was mainly attributed to the adsorption of total dissolved N by RB-PRB. However, interception of TN from sloping farmland was not significantly enhanced when the RB-PRB width was >20 cm.

3.4 Total nitrogen content in soil of sloping farmland

The results of soil TN content in each treatment plot at different times during the whole experiment are shown in Figure 7. TN in the original soil measured in April 2019 was 2,316 mg kg^{-1}, at the beginning of the experiment. The TN content in the soil varied significantly with the seasons, showing a trend of high levels in autumn and winter and low levels in spring and summer. Compared with the CK, the effect of treatment VFS0 with only VFS setting was not significant on soil TN nutrients. As the width of RB-PRB increased, the soil TN content in VFS1, VFS2, VFS3, and VFS4 treatments gradually increased. The TN content of the VFS4 group measured in January 2020 was 3,898 mg kg^{-1}, which was 41.69% higher than that of CK group 2,751 mg kg^{-1}.

4 Discussion

4.1 Mechanism of nitrate and ammonium N adsorption by biochar

The sorption of NO_3^--N and NH_4^+-N on biochar was better described by the Langmuir equation (R_L^2 = 0.9588 and 0.9673) than the Freundlich equation (R_F^2 = 0.8812 and 0.9450). The Langmuir model describes the adsorption by a monolayer, whereas the Freundlich model describes non-homogeneous adsorption. The better fitting results of NO_3^--N and NH_4^+-N by the Langmuir

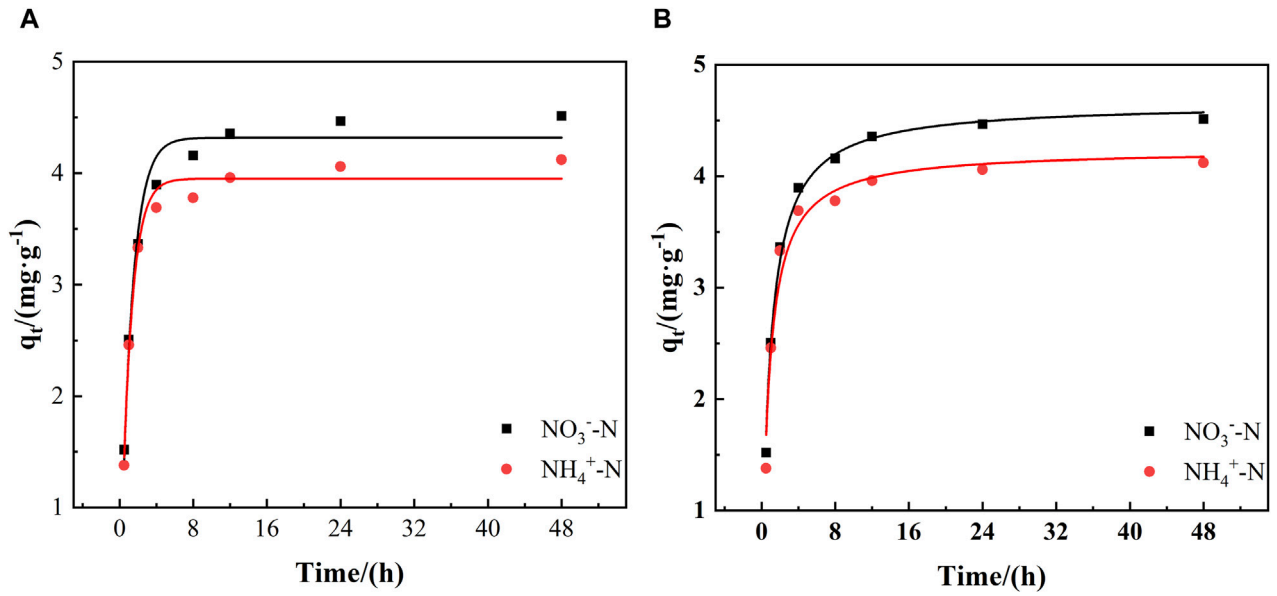

FIGURE 4
Kinetic adsorption of NO_3^--N and NH_4^+-N on biochar fitted using pseudo-first-order **(A)** and pseudo-second-order **(B)** equations.

TABLE 2 Kinetic parameters of NO_3^--N and NH_4^+-N adsorption on biochar.

	Actual equilibrium adsorption/mg·g^{-1}	Pseudo-first-order			Pseudo-second-order		
		q_e/mg·g^{-1}	k_1/h^{-1}	R^2	q_e/mg·g^{-1}	k_2/g·(mg·h)$^{-1}$	R^2
NO_3^--N	4.51	4.32	0.8067	0.9747	4.66	0.2452	0.9916
NH_4^+-N	4.12	3.95	0.9157	0.9805	4.24	0.3093	0.9654

equation indicate that adsorption of NO_3^--N and NH_4^+-N is dominated by consistent with monolayer physical adsorption (Kizito et al., 2015). Shin et al. observed that NH_4^+ was adsorbed rapidly on biochar pellets comprised of 9:1 biochar pellet:pig manure based on kinetic models (Shin et al., 2018). Biochar and agricultural residues, such as rice husks or plant shells, exhibit an ammonium removal efficiency of less than 40% at maximum (Kizito et al., 2015). This is consistent with the results of this study, indicating that biochar has the potential to rapidly adsorb N from runoff due to its large specific surface area. The maximum adsorption of NO_3^--N and NH_4^+-N by biochar in this study was 6.04 and 4.10 mg g^{-1} according to the Langmuir model, which is not very similar compared to some studies. Zhang et al. found that the maximum adsorption of NO_3^--N by iron-based biochar was 9.35 mg g^{-1} (Zhang et al., 2023). Although NO_3^--N and NH_4^+-N sorption capacity can be increased by active modification through metal ions or acids and bases, biochar modified in such a way may not be suitable for agricultural purposes due to potential environmental impacts (Yao et al., 2012; Liu Z. et al., 2016). In the Freundlich model, the absorption constants 1/n for both NO_3^--N and NH_4^+-N were less than 1, indicating a favorable process. The results suggest that the biochar surface is heterogeneous, with some level of physical adsorption taking place (Liu et al., 2010). The constant values ($0 < 1/n < 1$) indicate that the sorption process primarily involves chemical adsorption with slight physical adsorption (Yao et al., 2013).

Biochar adsorption of NO_3^--N and NH_4^+-N reached an apparent adsorption equilibrium after 12 h. As evidenced by their regression coefficients (R), the pseudo-first-order and pseudo-second-order models could be used to fit the adsorption data well. Previous studies found that a pseudo-second-order model was suitable for describing NO_3^--N and NH_4^+-N adsorption on biochar (Liu et al., 2010; Wang et al., 2019). This suggests also that the adsorption of NO_3^--N and NH_4^+-N by biochar can be a consequence of the combined mechanisms of physical and chemical adsorption, encompassing surface adsorption and intraparticle diffusion (Stjepanović et al., 2019). The adsorption mechanism of NO_3^--N and NH_4^+-N on biochar can be elucidated as follows: a rapid adsorption phase within the initial period (0–12 h) where over 85% of the maximum adsorption capacity for NO_3^--N and NH_4^+-N can be observed. This rapid adsorption is primarily a physical process driven by mass transfer based on the ionic concentration gradient between the solid and liquid phases, coupled with electrostatic interactions between positively charged radicals and negatively charged biochar surfaces (Zhu et al., 2012). Subsequently, a slower adsorption phase seem to occur, marking the conclusion of physical adsorption (12–48 h). This may imply that an ionic equilibrium between the solid and liquid phases, leading to

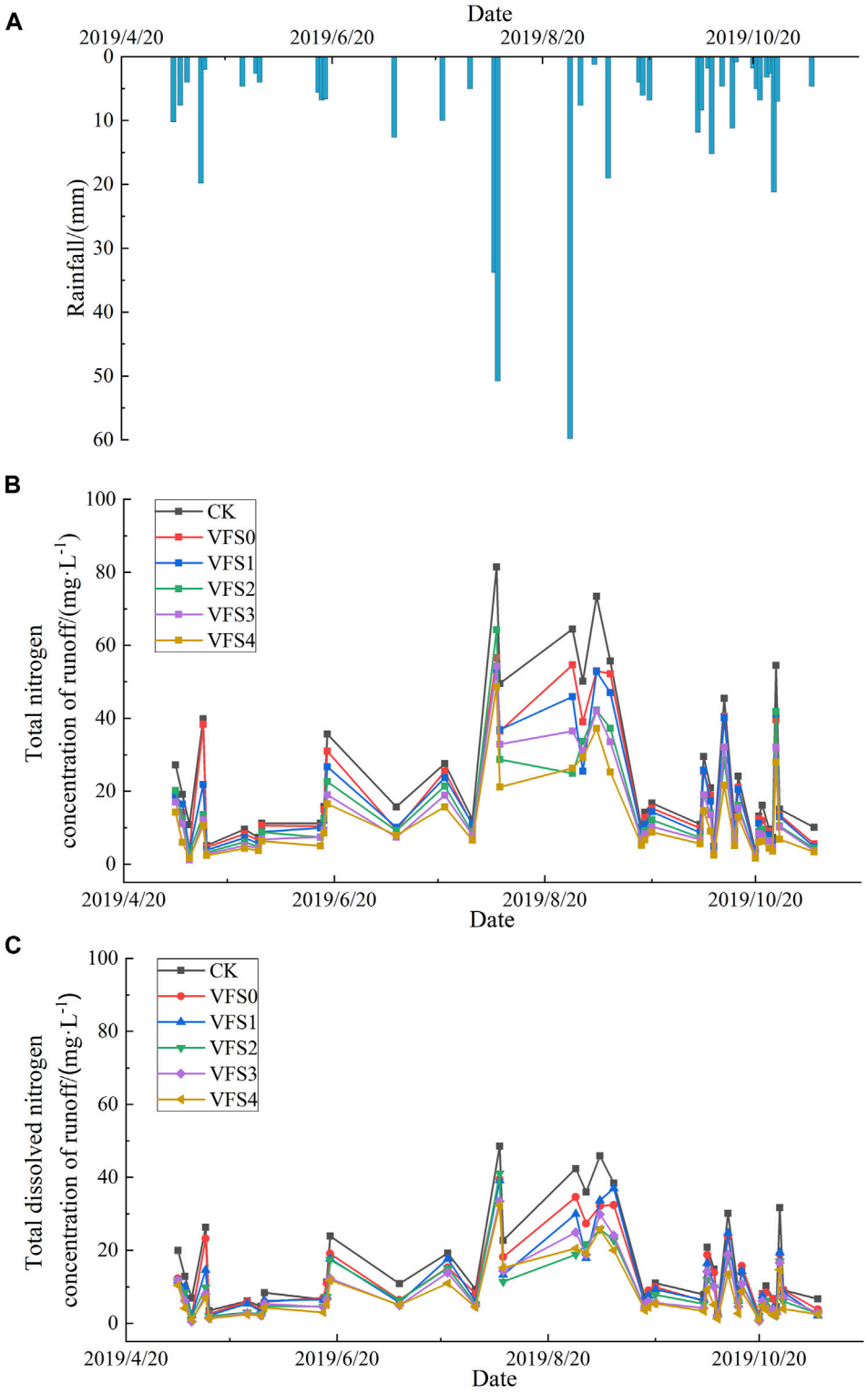

FIGURE 5
Time series of precipitation **(A)**, TN concentrations **(B)** and TDN concentrations **(C)** in runoff from sloping farmland. Precipitation and runoff are directly corresponding to each other. CK stands for untreated. VFS stands for Vegetation Filter Strip for this treatment, followed by the numbers 0, 1, 2, 3, and 4, which represent the width of the RB-PRB of 0 m, 0.1 m, 0.2 m, 0.3 m, and 0.4 m, respectively. RB-PRB stands for ridged biochar permeable reactive barrier.

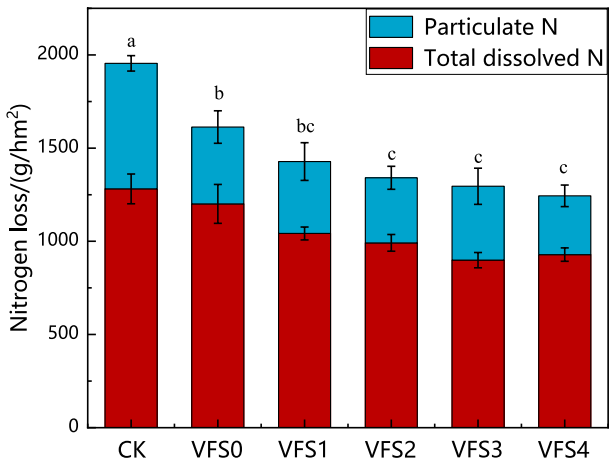

FIGURE 6
Particulate nitrogen and total dissolved nitrogen loss fluxes in runoff plots from sloping farmland under RB-PRB with VFS at different widths. CK stands for untreated. VFS stands for Vegetation Filter Strip for this treatment, followed by the numbers 0, 1, 2, 3, and 4, which represent the width of the RB-PRB of 0 m, 0.1 m, 0.2 m, 0.3 m, and 0.4 m, respectively. RB-PRB stands for ridged biochar permeable reactive barrier. PN stands for particulate nitrogen. TDN stands for total dissolved nitrogen. Different lowercase letters in the same figure indicate significant differences among the different plantation ages in the same soil layer at the 0.05 level.

minor desorption of physically bound NO_3^--N and NH_4^+-N. The enhanced adsorption during this phase is attributable to chemisorption and a degree of intranodal diffusion, continuing until the saturation of active sites (Kucic et al., 2013). Both equilibrium and kinetic data suggest that the adsorption mechanisms for both NO_3^--N and NH_4^+-N on biochar are dominated by rapid physical adsorption. This makes RB-PRB suitable for rapid adsorption of N from subsurface runoff from sloping farmland, but there may be desorption problems that need to be further explored.

4.2 Effect of RB-PRB with VFS on nitrogen loss from sloping farmland

In this investigation, it was found that nitrogen loss in sloping farmland was mainly in the form of dissolved N. The loss of soil N via runoff pathways, including overland flow and interflow, involves an interactive process between soil N and runoff water (Wang and Zhu, 2011). N is highly mobile and can be easily transported by both pathways. Interflow has been reported as the predominant pathway for NO_3^--N loss from sloping farmland (Jia et al., 2007), although conflicting results have been obtained in other studies (Chen et al., 2024). In this study, TDN was identified as the primary form of N loss from sloping farmland. Jing et al. found that dissolved organic N accounted for a significant proportion of TN loss via surface runoff and interflow, ranging from 24.31% to 57.69% and from 12.28% to 47.81%, respectively, which is consistent with the conclusions of this study (Jing et al., 2022). This also indicates that controlling the loss of TDN in subsurface runoff can be the key to intercept N loss from sloping farmland in the southwest.

It was found that RB-PRB with VFS in sloping farmland can intercept N via adsorption from surface runoff and subsurface runoff. Previous studies assessing the effectiveness of vegetated filter strips (VFS) in limiting nutrient transport to surface waters

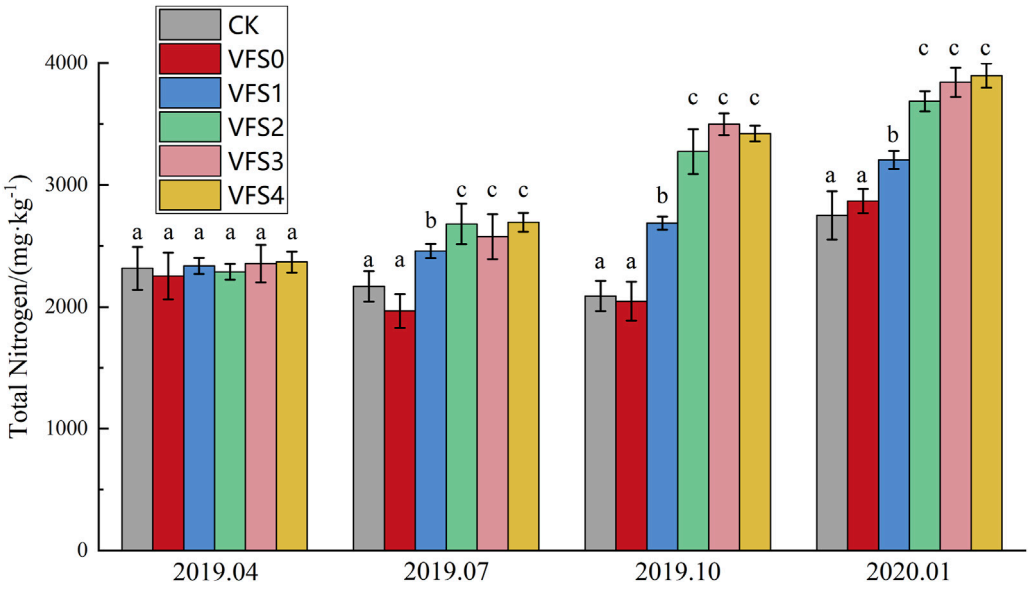

FIGURE 7
Time series of total nitrogen content in soil of sloping farmland under RB-PRB with VFS at different widths. CK stands for untreated. VFS stands for Vegetation Filter Strip for this treatment, followed by the numbers 0, 1, 2, 3, and 4, which represent the width of the RB-PRB of 0 m, 0.1 m, 0.2 m, 0.3 m, and 0.4 m, respectively. RB-PRB stands for ridged biochar permeable reactive barrier. Different lowercase letters in the same figure indicate significant differences among the different plantation ages in the same soil layer at the 0.05 level.

have typically examined various forms of N (Alemu et al., 2017). As Harmel et al. reported, VFS significantly reduced total N from swine feedlots by 81%–86% over a 4-year study, but less effectively trapped nitrate, which is the most total dissolved form of N (Harmel et al., 2018). The effectiveness of VFS in removing suspended solids explains why sediment-bound forms of nutrients are efficiently removed, and why TN removal is positively correlated with suspended solids removal (Yang et al., 2015; Alemu et al., 2017). The literature suggests that VFS may struggle to reduce the movement of more total dissolved forms of N (e.g., nitrate) and P into surface waters, although relatively high trapping efficiencies have been reported for these forms (Yang et al., 2015). In a recent study, Tang et al. evaluated the long-term effectiveness of different types and lengths of VFS in reducing suspended solids and nutrients in agricultural runoff (Tang et al., 2021). They found that VFS (9 m, 13 m) reduced suspended solids to 79% and 84% of the original amount, in consistence with the findings of the present study.

Our results suggest that the best control of N loss was achieved with an RB-PRB width of 0.3 m. Increasing the width further led to a decrease in interception effect, possibly due to excessive biochar application leading to increased biological fixation of N and reduced availability of plant N (Wu et al., 2022). This can be detrimental to the growth of Hybrid Giant Napier and can result in grass root rot. Meanwhile, agricultural residues decay and enter runoff with rainwater, which may positively impact soil erosion resistance but negatively affect soil retention (Hu et al., 2019). For instance, Wu et al. reported that while the inhibition of soil erosion was greatest at a biochar content of 50 t hm^{-2}, the amount of N loss associated with eroded soil doubled when the biochar content exceeded this level (Wu et al., 2022). In conclusion, RB-PRB with VFS was effective for controlling N loss from sloping farmland.

4.3 Effect of RB-PRB with VFS on soil nutrients in sloping farmland

The effects of RB-PRB with VFS on soil nutrient content are complex (Ali et al., 2020). Numerous studies have demonstrated that biochar enhances soil physical properties, but the influence of biochar on soil erosion remains unclear and inconsistent (Jeffery et al., 2011; Burrell et al., 2016; Głąb et al., 2016). Our current study showed that RB-PRB with VFS significantly increased soil TN content in sloping farmland. This is related to the effect of this interception zone on trapping nutrient loss from sloping farmland, which allows nitrogen to accumulate in the soil (Yadav et al., 2019). Meanwhile, this also suggests that biochar may be beneficial for soil nutrient retention. As previously indicated, biochar can boost soil microbial populations, enhance soil pH, stimulate soil enzyme activity, and increase porosity and macro-aggregates. Applied at optimal rates in agricultural production, biochar is effective in reducing soil erosion and promoting nutrient accumulation (Kuoppamaki et al., 2016; Sadeghi et al., 2016).

Other studies have shown that N leaching from soils can be significantly reduced by moderate application of biochar, and field experiments showed that leaching of ammonia and nitrate N from sandy soils was effectively reduced by 14% and 28% respectively when biochar was added at 25 t hm^{-2} in the 1–10 cm topsoil layer (Wu et al., 2022). This could be because the high specific surface area and porosity of biochar in RB-PRB can promote soil microbial and plant root growth, leading to enhanced soil microbial reproduction, enzyme activity, and nutrient cycling. As a result, soil fertility and crop yield may indirectly improve (Igalavithana et al., 2016; Wang et al., 2016).

Moreover, with a further increase in RB-PRB width to >0.2 m, the effect of N increase in soil was not significant, and even decreased at the larger widths. This may be due to quantities of volatile matter in biochar resulting in a high soil C/N ratio, which could have reduced soil fixation of N, inhibits soil N cycling, and leads to reduced N uptake by roots (Jost et al., 2011). Additionally, excessive biochar resulted in poor root development in Hybrid giant napier, increasing the likelihood of sediment and nitrogen loss. This may be due to the negative effect of poor Hybrid giant napier growth on biological soil particle aggregation, which alters the soil physical structure, adversely affects soil consistency, accelerates the soil nitrification process, and increases NO_3^- content in soil (Ye et al., 2012; Hui et al., 2014).

5 Conclusion

In the laboratory experiments conducted within the presented study, isothermal adsorption equilibrium and adsorption kinetic data demonstrated that rapid physical adsorption was the main adsorption mechanism for NO_3^--N and NH_4^+-N on biochar. This suggests that biochar has the potential to rapidly adsorb nutrients from slope-following ground runoff. Field experiments showed that N loss from the sloping farmland varied significantly with seasons, indicating a trend of high levels in summer and low levels in winter. The main pathway of TN loss was TDN runoff through subsurface flow. The investigation of TN loss from runoff plots revealed that the TN loss in the control group was 1954 g·hm^{-2}. However, incorporating RB-PRB with VFS notably decreased N loss from sloping cultivated land. When the width was 0.3 m, RB-PRB with VFS intercepted 34.85% of N, with little change in effectiveness with increased width. The efficiency of intercepting particulate nitrogen was 32.75% for the treatment in which only VFS was set. During the experimental period, RB-PRB with VFS significantly increased the TN content in the soil of the sloping farmland site, with a maximum increase of 41.69% compared to the control. These results demonstrate the potential of RB-PRB with VFS in reducing N loss and improving soil stability, offering a solution for mitigating N loss from sloping farmland. Nevertheless, further experiments are still required to explore the adsorption capacity of biochar and plant harvesting for VFS.

Data availability statement

The original contributions presented in the study are included in the article/Supplementary Material, further inquiries can be directed to the corresponding author.

Author contributions

YZ: Writing–original draft, Methodology, Investigation, Formal Analysis. JG: Writing–review and editing, Methodology, Formal

Analysis. QL: Writing–review and editing, Conceptualization, Methodology. SZ: Writing–review and editing, Supervision, Investigation, Funding acquisition, Formal Analysis, Conceptualization.

Funding

The author(s) declare financial support was received for the research, authorship, and/or publication of this article. This work was financially supported by grants from the Guangxi Key Laboratory of Superior Timber Trees Resource Cultivation (Grant number 22-B-01-03) and the National Key Research and Development Project (Grant number 2017YFD0800505).

Acknowledgments

The authors are thankful to Institute of Mountain and Environment, Chinese Academy of Sciences for providing us with Test site and laboratory during the research project.

Conflict of interest

The authors declare that the research was conducted in the absence of any commercial or financial relationships that could be construed as a potential conflict of interest.

Publisher's note

Supplementary material

The Supplementary Material for this article can be found online at: https://www.frontiersin.org/articles/10.3389/fenvs.2024.1381781/full#supplementary-material

References

Alemu, T., Bahrndorff, S., Alemayehu, E., and Ambelu, A. (2017). Agricultural sediment reduction using natural herbaceous buffer strips: a case study of the east African highland. *Water Environ. J.* 31 (4), 522–527. doi:10.1111/wej.12274

Ali, I., Ullah, S., He, L., Zhao, Q., Iqbal, A., Wei, S., et al. (2020). Combined application of biochar and nitrogen fertilizer improves rice yield, microbial activity and N-metabolism in a pot experiment. *PeerJ.* 13 (8), e10311. doi:10.7717/peerj.10311

Burrell, L. D., Zehetner, F., Rampazzo, N., Wimmer, B., and Soja, G. (2016). Long-term effects of biochar on soil physical properties. *Geoderma* 282, 96–102. doi:10.1016/j.geoderma.2016.07.019

Chen, C., Deng, H., Xin, G., and Zhou, Y. (2024). Characteristics of nitrogen and phosphorus contents in soil and water in an agricultural catchment of the three Gorges reservoir area. *Front. Environ. Sci.* 11. doi:10.3389/fenvs.2023.1327260

Chen, L., Wang, L., Lu, X., Yin, Q., and Liu, D. (2022). Utilization of plant litter to enhance the effect of lakebank on nitrogen interception/removal from runoff: a microcosm simulation study. *Environ. Eng. Sci.* 39 (3), 235–247. doi:10.1089/ees.2021.0098

Chen, X., Zhou, B., Wang, Q., Tao, W., and Lin, H. (2020). Nano-biochar reduced soil erosion and nitrate loss in sloping fields on the Loess Plateau of China. *Catena* 187, 104346. doi:10.1016/j.catena.2019.104346

Dai, X., Xiao, X., Dai, W., Liu, S., Dong, X., and Shen, R. et al (2023). Comparison of nitrate and ammonium leaching of soils collected from different regions of China: a soil column experiment. *J. Soil Sci. Plant Nutr.* 23, 6059–6070. doi:10.1007/s42729-023-01464-4

Gene, S., Hoekstra, P., Hannam, C., White, M., Truman, C., and Hanson, M. et al (2019). The role of vegetated buffers in agriculture and their regulation across Canada and the United States. *J. Environ. Manag.* 243, 12–21. doi:10.1016/j.jenvman.2019.05.003

Głąb, T., Palmowska, J., Zaleski, T., and Gondek, K. (2016). Effect of biochar application on soil hydrological properties and physical quality of sandy soil. *Geoderma* 281, 11–20. doi:10.1016/j.geoderma.2016.06.028

Guo, S., Zhai, L., Liu, J., Liu, H., Chen, A., and Wang, H. et al (2019). Cross-ridge tillage decreases nitrogen and phosphorus losses from sloping farmlands in southern hilly regions of China. *Soil Tillage Res.* 191, 48–56. doi:10.1016/j.still.2019.03.015

Harmel, R. D., Pampell, R., Gentry, T., Smith, D. R., Hajda, C., and Wagner, K. et al (2018). Vegetated treatment area (VTAs) efficiencies for *E. coli* and nutrient removal on small-scale swine operations. *Int. Soil Water Conservation Res.* 6 (2), 153–164. doi:10.1016/j.iswcr.2018.02.002

He, Z., Wang, C., Cao, H., Liang, J., Pei, S., and Li, Z. (2023). Nitrate absorption and desorption by biochar. *Agronomy* 13, 2440. doi:10.3390/agronomy13092440

Holly, M. A., Larson, R. A., Cooley, E. T., and Wunderlin, A. M. (2018). Silage storage runoff characterization: annual nutrient loading rate and first flush analysis of bunker silos. *Agric. Ecosyst. Environ.* 264, 85–93. doi:10.1016/j.agee.2018.05.015

Hu, X. D., Zhang, H. Y., Liu, Q. J., Xu, X. Z., Qiu, D. X., and Ma, L. (2019). Impact of furrow slopes on losses of dissolved nitrogen and phosphorus under simulated rainfall. *J. Soil Water Conserv.* 33 (6), 41–46. doi:10.13870/j.cnki.stbcxb.2019.06.006

Huang, R., Gao, X., Wang, F., Xu, G., Long, Y., and Wang, C. et al (2020). Effects of biochar incorporation and fertilizations on nitrogen and phosphorus losses through surface and subsurface flows in a sloping farmland of Entisol. *Agric. Ecosyst. Environ.* 300, 106988. doi:10.1016/j.agee.2020.106988

Huang, R., Tian, D., Liu, J., Lv, S., He, X., and Gao, M. (2018). Responses of soil carbon pool and soil aggregates associated organic carbon to straw and straw-derived biochar addition in a dryland cropping mesocosm system. *Agric. Ecosyst. Environ.* 265, 576–586. doi:10.1016/j.agee.2018.07.013

Hui, J., Zhang, A., Liu, R., Wang, Y., Chen, Z., and Yang, Z. (2014). Effects of biochar on soil nutrients and nitrogen leaching in anthropogenic-alluvial soil. *Chin. J. Agrometeorology* 35 (2), 156–161. doi:10.3969/j.issn.1000-6362.2014.02.006

Ibrikci, H., Cetin, M., Karnez, E., Flügel, W. A., Tilkici, B., and Bulbul, Y. et al (2015). Irrigation-induced nitrate losses assessed in a Mediterranean irrigation district. *Agric. Water Manag.* 148, 223–231. doi:10.1016/j.agwat.2014.10.007

Igalavithana, A. D., Ok, Y. S., Usman, A. R. A., Al-Wabel, M. I., Oleszczuk, P., and Lee, S. S. (2016). The effects of biochar amendment on soil fertility. *Agric. Environ. Appl. Biochar Adv. Barriers*, 123–144. doi:10.2136/sssaspecpub63.2014.0040

James, R., and Haby, V. (1971). Simplified colorimetric determination of soil organic matter. *Soil Sci.* 112, 137–141. doi:10.1097/00010694-197108000-00007

Janssen, M., Frings, J., and Lennartz, B. (2018). Effect of grass buffer strips on nitrate export from a tile-drained field site. *Agric. Water Manag.* 208, 318–325. doi:10.1016/j.agwat.2018.06.026

Jeffery, S., Verheijen, F. G. A., van der Velde, M., and Bastos, A. C. (2011). A quantitative review of the effects of biochar application to soils on crop productivity using meta-analysis. *Agric. Ecosyst. Environ.* 144 (1), 175–187. doi:10.1016/j.agee.2011.08.015

Jia, H., Lei, A., Lei, J., Ye, M., and Zhao, J. (2007). Effects of hydrological processes on nitrogen loss in purple soil. *Agric. Water Manag.* 89 (1), 89–97. doi:10.1016/j.agwat.2006.12.013

Jing, X., Li, L., Chen, S., Shi, Y., Xu, M., and Zhang, Q. (2022). Straw returning on sloping farmland reduces the soil and water loss via surface flow but increases the nitrogen loss via interflow. *Agric. Ecosyst. Environ.* 339, 108154. doi:10.1016/j.agee.2022.108154

Jost, G., Dirnböck, T., Grabner, M.-T., and Mirtl, M. (2011). Nitrogen leaching of two forest ecosystems in a karst watershed. *Water, Air, & Soil Pollut.* 218 (1), 633–649. doi:10.1007/s11270-010-0674-8

Kizito, S., Wu, S., Kipkemoi Kirui, W., Lei, M., Lu, Q., and Bah, H. et al (2015). Evaluation of slow pyrolyzed wood and rice husks biochar for adsorption of ammonium

nitrogen from piggery manure anaerobic digestate slurry. *Sci. Total Environ.* 505, 102–112. doi:10.1016/j.scitotenv.2014.09.096

Kucic, D., Cosic, I., Vukovic, M., and Briski, F. (2013). Sorption kinetic studies of ammonium from aqueous solution on different inorganic and organic media. *Acta Chim. Slov.* 60, 109–119.

Kuoppamaki, K., Hagner, M., Lehvavirta, S., and Setala, H. (2016). Biochar amendment in the green roof substrate affects runoff quality and quantity. *Ecol. Eng.* 88, 1–9. doi:10.1016/j.ecoleng.2015.12.010

Lee, C., Wang, C., Lin, H., Lee, S., Tsang, D., and Jien, S. et al (2018). *In-situ* biochar application conserves nutrients while simultaneously mitigating runoff and erosion of an Fe-oxide-enriched tropical soil. *Sci. Total Environ.* 619-620, 665–671. doi:10.1016/j.scitotenv.2017.11.023

Lemma, B., Kebede, F., Mesfin, S., Fitiwy, I., Abraha, Z., and Norgrove, L. (2017). Quantifying annual soil and nutrient lost by rill erosion in continuously used semiarid farmlands, North Ethiopia. *Environ. Earth Sci.* 76 (5), 190. doi:10.1007/s12665-017-6506-z

Li, T., Zhang, Y., He, B., Wu, X., and Du, Y. (2022). Nitrate loss by runoff in response to rainfall amount category and different combinations of fertilization and cultivation in sloping croplands. *Agric. Water Manag.* 273, 107916. doi:10.1016/j.agwat.2022.107916

Libutti, A., and Monteleone, M. (2017). Soil vs. groundwater: the quality dilemma. Managing nitrogen leaching and salinity control under irrigated agriculture in Mediterranean conditions. *Agric. Water Manag.* 186, 40–50. doi:10.1016/j.agwat.2017.02.019

Liu, H., Dong, Y., Liu, Y., and Wang, H. (2010). Screening of novel low-cost adsorbents from agricultural residues to remove ammonia nitrogen from aqueous solution. *J. Hazard. Mater.* 178 (1), 1132–1136. doi:10.1016/j.jhazmat.2010.01.117

Liu, H., Wang, Y., and Tang, M. (2017). Arbuscular mycorrhizal fungi diversity associated with two halophytes lycium barbarum L. And elaeagnus angustifolia L. In ningxia, China. *Arch. Agron. Soil Sci.* 63, 796–806. doi:10.1080/03650340.2016.1235783

Liu, Y.-J., Yang, J., Hu, J.-M., Tang, C.-J., and Zheng, H.-J. (2016a). Characteristics of the surface–subsurface flow generation and sediment yield to the rainfall regime and land-cover by long-term *in-situ* observation in the red soil region, Southern China. *J. Hydrology* 539, 457–467. doi:10.1016/j.jhydrol.2016.05.058

Liu, Z., Xue, Y., Gao, F., Cheng, X., and Yang, K. (2016b). Removal of ammonium from aqueous solutions using alkali-modified biochars. *Chem. Speciat. Bioavailab.* 28 (1-4), 26–32. doi:10.1080/09542299.2016.1142833

Losacco, D., Ancona, V., De Paola, D., Tumolo, M., Massarelli, C., and Gatto, A. et al (2021). Development of ecological strategies for the recovery of the main nitrogen agricultural pollutants: a review on environmental sustainability in agroecosystems. *Sustainability* 13, 7163. doi:10.3390/su13137163

Luo, H., Li, X., Chen, Y., Liu, X., Zhang, K., Fu, X., et al. (2022). Field engineering application of agricultural farmland surface runoff pollution treatment by combined bioreactor and constructed wetlands. *Int. J. Environ. Sci. Technol.* 19 (6), 5493–5510. doi:10.1007/s13762-021-03449-1

Lyu, C., Li, X., Yuan, P., Song, Y., Gao, H., and Liu, X. et al (2021). Nitrogen retention effect of riparian zones in agricultural areas: a meta-analysis. *J. Clean. Prod.* 315, 128143. doi:10.1016/j.jclepro.2021.128143

Peng, X., Dai, Q., Ding, G., and Li, C. (2019). Role of underground leakage in soil, water and nutrient loss from a rock-mantled slope in the karst rocky desertification area. *J. Hydrology* 578, 124086. doi:10.1016/j.jhydrol.2019.124086

Peng, X., Zhu, Q. H., Xie, Z. B., Darboux, F., and Holden, N. M. (2016). The impact of manure, straw and biochar amendments on aggregation and erosion in a hillslope Ultisol. *Catena* 138, 30–37. doi:10.1016/j.catena.2015.11.008

Prosser, R. S., Hoekstra, P. F., Gene, S., Truman, C., White, M., and Hanson, M. L. (2020). A review of the effectiveness of vegetated buffers to mitigate pesticide and nutrient transport into surface waters from agricultural areas. *J. Environ. Manag.* 261, 110210. doi:10.1016/j.jenvman.2020.110210

Ruan, L., Wei, K., Wang, L., Cheng, H., Zhang, F., Wu, L., et al. (2016). Characteristics of NH4+ and NO3− fluxes in tea (Camellia sinensis) roots measured by scanning ion-selective electrode technique. *Sci. Rep.* 6 (1), 38370. doi:10.1038/srep38370

Sadeghi, S. H., Hazbavi, Z., and Harchegani, M. K. (2016). Controllability of runoff and soil loss from small plots treated by vinasse-produced biochar. *Sci. Total Environ.* 541, 483–490. doi:10.1016/j.scitotenv.2015.09.068

Shen, W., Li, S., Mi, M., Zhuang, Y., and Zhang, L. (2021). What makes ditches and ponds more efficient in nitrogen control? *Agric. Ecosyst. Environ.* 314, 107409. doi:10.1016/j.agee.2021.107409

Shin, J., Choi, E., Jang, E., Hong, S. G., Lee, S., and Ravindran, B. (2018). Adsorption characteristics of ammonium nitrogen and plant responses to biochar pellet. *Sustainability* 10 (5), 1331. doi:10.3390/su10051331

Stjepanović, M., Velić, N., Lončarić, A., Gašo-Sokač, D., Bušić, V., and Habuda-Stanić, M. (2019). Adsorptive removal of nitrate from wastewater using modified lignocellulosic waste material. *J. Mol. Liq.* 285, 535–544. doi:10.1016/j.molliq.2019.04.105

Tang, J., Zhu, Y., Wei, Z., Feng, L., Yang, N., and Sun, Z. et al (2021). Effectiveness of riparian vegetated filter strips in removing agricultural nonpoint source pollutants in agricultural runoff from the liao river area, China. *Pol. J. Environ. Stud.* 30 (5), 4709–4718. doi:10.15244/pjoes/133720

Tsiknia, M., Tzanakakis, V., Oikonomidis, D., Paranychianakis, N., and Nikolaidis, N. (2014). Effects of olive mill wastewater on soil carbon and nitrogen cycling. *Appl. Microbiol. Biotechnol.* 98, 2739–2749. doi:10.1007/s00253-013-5272-4

Tuo, D., Xu, M., and Gao, G. (2018). Relative contributions of wind and water erosion to total soil loss and its effect on soil properties in sloping croplands of the Chinese Loess Plateau. *Sci. Total Environ.* 633, 1032–1040. doi:10.1016/j.scitotenv.2018.03.237

Wang, H., Gao, L., Pang, Z., Yang, J., Chen, X., Zhang, J., et al. (2022). Surface flow–interflow-coupled nitrogen loss in gray fluvo-aquic farmland soils in the Anhui Section of the Huaihe River Basin, China. *Can. J. Soil Sci.* 102 (2), 331–340. doi:10.1139/cjss-2021-0122

Wang, J., Xiong, Z., and Kuzyakov, Y. (2016). Biochar stability in soil: meta-analysis of decomposition and priming effects. *GCB Bioenergy* 8 (3), 512–523. doi:10.1111/gcbb.12266

Wang, T., and Zhu, B. (2011). Nitrate loss via overland flow and interflow from a sloped farmland in the hilly area of purple soil, China. *Nutrient Cycl. Agroecosyst.* 90 (3), 309–319. doi:10.1007/s10705-011-9431-7

Wang, W., Maimaiti, A., Shi, H., Wu, R., Wang, R., Li, Z., et al. (2019). Adsorption behavior and mechanism of emerging perfluoro-2-propoxypropanoic acid (GenX) on activated carbons and resins. *Chem. Eng. J.* 364, 132–138. doi:10.1016/j.cej.2019.01.153

Wang, X., Li, J., Li, S., and Zheng, X. (2017). A study on removing nitrogen from paddy field rainfall runoff by an ecological ditch–zeolite barrier system. *Environ. Sci. Pollut. Res.* 24 (35), 27090–27103. doi:10.1007/s11356-017-0269-7

Wang, Y., Chen, F., Zhao, H., Xie, D., Ni, J., and Liao, D. (2023). Characteristics of agricultural phosphorus migration in different soil layers on purple soil sloping cropland under natural rainfall conditions. *Front. Environ. Sci.* 11, 1230565. doi:10.3389/fenvs.2023.1230565

Wei, D., Singh, R. P., Li, Y., and Fu, D. (2020). Nitrogen removal efficiency of surface flow constructed wetland for treating slightly polluted river water. *Environ. Sci. Pollut. Res.* 27 (20), 24902–24913. doi:10.1007/s11356-020-08393-0

Wu, L., Liu, X., Yu, Y., and Ma, X. (2022). Biochar, grass, and cross-ridge reshaped the surface runoff nitrogen under consecutive rainstorms in loessial sloping lands. *Agric. Water Manag.* 261, 107354. doi:10.1016/j.agwat.2021.107354

Wu, X., Wei, Y., Wang, J., Xia, J., Cai, C., and Wei, Z. (2018). Effects of soil type and rainfall intensity on sheet erosion processes and sediment characteristics along the climatic gradient in central-south China. *Sci. Total Environ.* 621, 54–66. doi:10.1016/j.scitotenv.2017.11.202

Xiang, G., Long, S., Liu, H., and Wu, X. (2021). Cd(II) removal from aqueous solutions by pomelo peel derived biochar in a permeable reactive barrier: modelling, optimization and mechanism. *Mater. Res. Express* 8, 115508. doi:10.1088/2053-1591/ac386b

Yadav, V., Karak, T., Singh, S., Singh, A., and Khare, P. (2019). Benefits of biochar over other organic amendments: responses for plant productivity (*Pelargonium graveolens L.*) and nitrogen and phosphorus losses. *Industrial Crops Prod.* 131, 96–105. doi:10.1016/j.indcrop.2019.01.045

Yang, F., Yang, Y., Li, H., and Cao, M. (2015). Removal efficiencies of vegetation-specific filter strips on nonpoint source pollutants. *Ecol. Eng.* 82, 145–158. doi:10.1016/j.ecoleng.2015.04.018

Yanu, P., and Jakmunee, J. (2015). Flow injection with in-line reduction column and conductometric detection for determination of total inorganic nitrogen in soil. *Talanta* 144, 263–267. doi:10.1016/j.talanta.2015.06.002

Yao, Y., Gao, B., Chen, J., and Yang, L. (2013). Engineered biochar reclaiming phosphate from aqueous solutions: mechanisms and potential application as a slow-release fertilizer. *Environ. Sci. Technol.* 47 (15), 8700–8708. doi:10.1021/es4012977

Yao, Y., Gao, B., Zhang, M., Inyang, M., and Zimmerman, A. R. (2012). Effect of biochar amendment on sorption and leaching of nitrate, ammonium, and phosphate in a sandy soil. *Chemosphere* 89 (11), 1467–1471. doi:10.1016/j.chemosphere.2012.06.002

Ye, L., Wang, C., Zhou, H., and Peng, X. (2012). Effects of rice straw-derived biochar addition on soil structure stability of an ultisol. *Soils* 44 (1), 62–66. doi:10.13758/j.cnki.tr.2012.01.009

Zhang, Z., Huang, G., Zhang, P., Shen, J., Wang, S., and Li, Y. (2023). Development of iron-based biochar for enhancing nitrate adsorption: effects of specific surface area, electrostatic force, and functional groups. *Sci. Total Environ.* 856, 159037. doi:10.1016/j.scitotenv.2022.159037

Zhao, P., Tang, X., Tang, J., and Zhu, B. (2015). The nitrogen loss flushing mechanism in sloping farmlands of shallow Entisol in southwestern China: a study of the water source effect. *Arabian J. Geosciences* 8 (12), 10325–10337. doi:10.1007/s12517-015-1983-4

Zhu, B., Wang, T., Kuang, F., Luo, Z., Tang, J., and Xu, T. (2009). Measurements of nitrate leaching from a hillslope cropland in the central sichuan basin, China. *Soil Sci. Soc. Am. J.* 73 (4), 1419–1426. doi:10.2136/sssaj2008.0259

Zhu, K., Fu, H., Zhang, J., Lv, X., Tang, J., and Xu, X. (2012). Studies on removal of NH_4^+-N from aqueous solution by using the activated carbons derived from rice husk. *Biomass Bioenergy.* 43, 18–25. doi:10.1016/j.biombioe.2012.04.005